Rheological Properties of Polypropylene/High-Density Polyethylene Blend Melts. I. Capillary Flow Properties

MITSUYOSHI FUJIYAMA[1,*] and YOUTOKU KAWASAKI[2]

[1]Polymer Development Laboratory, Research and Development Division, and [2]Quality Control Section, Resins Division, Tokuyama Soda Co., Ltd., Tokuyama-shi, Yamaguchi-ken 745, Japan

SYNOPSIS

Three kinds of isotactic polypropylenes (PP) with different melt flow indexes (MFIs) were melt-blended with three kinds of high-density polyethylenes (HDPE) with different MFI using a screw extruder, and the morphologies and capillary flow properties such as flow curve, entrance effect, Barus effect, and melt fracture were studied. When HDPE contents were 70 wt % or above and PP particles formed the disperse phase, the size of the particles decreased with decreasing viscosity of PP. When HDPE contents were 30 wt % or below and HDPE particles formed the disperse phase, the size of the particles was minimum when the viscosities of PP and HDPE were similar. The die swell ratios of the blends were higher than those of the components. On the other hand, the entrance correction coefficients of the blends were intermediate between those of the components. There was no correlation between the die swell ratio and the entrance correction coefficient. Therefore, it is not always appropriate to regard the entrance correction coefficient as a measure of melt elasticity in the case of inhomogeneous polymer systems such as PP/HDPE blend.

INTRODUCTION

Blends of isotactic polypropylene (PP) and high-density polyethylene (HDPE) are industrially widely used for the purpose of improving the impact strength and processability of PP and improving the environmental stress cracking resistance and processability of HDPE. Many studies have so far been done on the rheological properties of PP/HDPE blends.[1-17] They include flow curve,[1-6,8,9,13,16,17] die swell,[7,11,15-17] melt fracture,[6,16] recoverable shear strain,[8,14] normal stress,[13,14] stress-optical coefficient,[13] relaxation time,[14] relaxation spectrum,[7] dynamic viscoelasticity,[12] and morphology formation.[10]

The present article concerns systematic studies on morphologies and the capillary flow properties such as flow curve, entrance effect, Barus effect, and melt fracture for the blends composed of the combination of three kinds of PPs with different melt flow indexes (MFIs) and three kinds of HDPEs with different MFI. In the following article, the dynamic viscoelastic properties will be reported.

EXPERIMENTAL

Samples

The characteristics of the raw resins used in this experiment are shown in Table I. MFI was measured using a counter method at 230°C under a load of 2160 g according to the ASTM D 1238-86T and was converted on PP volume. Molecular weights were measured at 135°C with a gel permeation chromatograph GPC 150-C manufactured by Waters Ltd. The column system used was 10^3, 10^4, 10^5, 10^6, and 10^7 Å and solvent used was *o*-dichlorobenzene. The last letters H, M, and L in the sample code indicate high, medium, and low MFI. PPH, PPM, PPL, PEH, and PEM have similar molecular weight distributions and PEL has a very broad distribution.

For the combination of PPM and three PEs and the combination of PEM and three PPs, both components were mixed with a tumbler to achieve com-

* To whom correspondence should be addressed.

Journal of Applied Polymer Science, Vol. 42, 467–480 (1991)
 CCC 0021-8995/91/020467-14$04.00

Table I Characteristics of Base Resins

Sample Code	Grade	Manufacturer	MFI (dg/min)	M_n ($\times 10^3$)	M_w ($\times 10^4$)	M_z ($\times 10^5$)	$\frac{M_w}{M_n}$	$\frac{M_z}{M_w}$
PPH	MJ160	Tokuyama Soda	27.3	22.5	18.4	8.6	8.2	4.7
PPM	YE130	Tokuyama Soda	4.6	35.9	29.6	12.3	8.3	4.1
PPL	RB110	Tokuyama Soda	0.51	75.0	57.3	17.4	7.6	3.0
PEH	JX-10	Mitsubishi Yuka	31.7	6.9	5.1	3.0	7.3	5.9
PEM	JX-20	Mitsubishi Yuka	7.6	9.2	7.6	4.0	8.3	5.2
PEL	5202B	Mitsui Petrochemical	0.26	10.3	15.2	9.8	14.8	6.4

positions of 0, 10, 30, 50, 70, 90, and 100 wt %. They were extruded and pelletized using a 40-mm ϕ single-screw extruder with an L/D of 22 and a compression ratio of 23 under conditions of cylinder and die temperatures of C_1 = 180°C, C_2 = 200°C, C_3 = 220°C, and D = 220°C and a screw revolution speed of 58 rpm. The same procedure was used for the samples of compositions of 0 and 100 wt %.

Morphology Observation

A few pellets were melted between two slide glasses on a hot plate whose temperature was 230°C, pressed gently to coalesce them to a thin sheet, held for 3 min, and cooled in air. The sheet crystallized about 40 s after it left the hot plate for all samples. A sheet about 0.5 mm thick was obtained. This sheet was cooled in liquid nitrogen and fractured. The fracture surface, onto which gold was vapor-deposited, was observed with a scanning electron microscope (SEM) JSM-T220 manufactured by JEOL Ltd.

Capillary Flow Properties

MFI was measured using a counter method with a melt indexer manufactured by Takara Kogyo Co., Ltd. at 230°C under a load of 2160 g according to the ASTM D 1238-86T and was converted on PP volume. After the extrudate solidified, its diameter D was measured with a micrometer, and the die swell ratio was evaluated by D/D_0 where D_0 was the capillary diameter.

The relation between pressure P and volumetric flow rate Q was measured at 230°C with a capillary rheometer, Koka Flow Tester manufactured by Shimazu Seisakusho Co., Ltd. using straight dies of a diameter $2R$ = 0.5 mm, lengths L = 1, 2.5, and 5 mm, and L/R = 4, 10, and 20.

The apparent shear stress τ'_w and the apparent shear rate $\dot{\gamma}'_w$ at the wall in capillary flow are given by Eqs. (1) and (2), respectively:

$$\tau'_w = \frac{PR}{2L} \tag{1}$$

$$\dot{\gamma}'_w = \frac{4Q}{\pi R^3} \tag{2}$$

If the entrance effect is corrected, the effective shear stress τ is given by Eq. (3)[18]:

$$\tau = \frac{PR}{2(L + \nu R)} \tag{3}$$

where ν is the end correction coefficient. If the non-Newtonianity of flow is corrected, the true shear rate $\dot{\gamma}$ is given by eq. (4)[19]:

$$\dot{\gamma} = \frac{\dot{\gamma}'_w}{4}\left(3 + \frac{d \log \dot{\gamma}'_w}{d \log \tau}\right) \tag{4}$$

The shear viscosity η is given by Eq. (5):

$$\eta = \frac{\tau}{\dot{\gamma}} \tag{5}$$

After the extrudate solidified, its diameter D at the part 5 mm from the front was measured with the micrometer and the ratio D/D_0 where D_0 is the capillary diameter was called die swell ratio and used as a measure of die well.

The appearance of the extrudate was observed with the naked eye and the occurrence of melt fracture was checked.

RESULTS AND DISCUSSION

Morphology

Figure 1(a) shows the variations, with PE content, of the SEM photographs of the fracture surfaces of PPM/PEH, PPM/PEM, and PPM/PEL blends.

It seems that particles observed in the blends with PE contents of 10 and 30 wt % are PE component, and particles observed in the blends with PE contents of 70 and 90 wt % are PP component. Interpenetrating inversion structures are observed in the blends with a PE content of 50 wt %. The size of the particles increases with increasing PE content, shows maxima at a PE content of 50 wt %, and after that, decreases with increasing PE content. Close inspection of the photographs shows that when PE contents are 50 wt % or above the size of the PP particles decreases with decreasing MFI (or increasing viscosity) of PE component, which is the disperse medium, and that when PE contents are 30 wt % or below the size of PE particles is the smallest for PPM/PEM blend whose components have similar MFIs. Figure 1(b) shows the SEM photographs of the fracture surfaces of PPH/PEM, PPM/PEM, and PPL/PEM blends. When PE contents are 70 wt % or above, the size of PP particles decreases with increasing MFI of PP. When PE contents are 30 wt % or below, the size of PE particles is the smallest for PPM/PEM blend whose components have similar MFIs.

Summarizing these results, when PE contents are 70 wt % or above and the PP particles form the disperse phase, the particle size decreases with decreasing viscosity of PP. When PE contents are 30 wt % or below and the PE particles form the disperse phase, the particle size is minimum when the viscosities of PP and PE are similar. Two cases have so far been reported on the particle size in various polymer blends. In one case the particle size is minimum when the viscosity ratio of both components is around unity.[20-27] In the other case the particle size decreases with decreasing viscosity of the disperse phase.[28-31] In the present experiment of PP/HDPE blends, the former behavior is observed when HDPE contents are 30 wt % or below and HDPE particles form the disperse phase, and the latter behavior is observed when HDPE contents are 70 wt % or above and PP particles form the disperse phase.

Melt Flow Index

Figure 2 shows the dependence of the MFIs of the blends on PE content. MFIs show positive deviations from logarithmic additivity and hence viscosities show negative deviations from logarithmic additivity. Many researchers[1-6,8,13] have already reported that the viscosities of PP/HDPE blends show negative deviations from logarithmic additivity.

Figure 3 shows the dependence of the die swell ratios at MFI measurement on PE content. The die swell ratio shows abnormally high values except for the case where either component has very low MFI (PPM/PEL and PPL/PEM). PPM/PEH and PPM/PEM show peaks at a PE content of 30 wt % and PPH/PEM shows two peaks at PE contents of 30 and 70 wt %. Shumskii[8] reported that the die swell ratio of PP/HDPE blend showed a positive deviation from additivity and showed a maximum at an HDPE content of around 50 wt %. Kasajima and Ito[15] found a maximum of the die swell ratio of PP/HDPE blend at an HDPE content of around 25 wt %.

Flow Curve

Figure 4 shows, as an example, the apparent flow curves ($\dot{\gamma}'_w - \tau'_w$) of PPM70/PEM30 obtained directly from the measured P and Q using Eqs. (1) and (2). Due to the entrance pressure loss, the apparent flow curve obtained with a die of smaller L/R locates at higher shear stress side.

Arranging eq. (3),

$$P = 2\tau(L/R) + 2\nu\tau \tag{6}$$

a straight line should be obtained if pressure P required to produce a definite shear stress τ, and hence a definite shear rate $\dot{\gamma}'_w$ is plotted against L/R (Bagley plot[18]), and the end correction coefficient ν is obtained as an intercept of L/R axis.

An example of the Bagley plot is shown in Figure 5 for PPM70/PEM30. Fine Bagley plots were obtained for all samples. The flow curve ($\dot{\gamma}'_w - \tau$) obtained by correcting the apparent shear stress τ'_w to the effective shear stress τ using Eq. (3) is also shown in Figure 4. Each flow curve with different L/R unites into one curve independent of L/R. The true flow curve ($\dot{\gamma} - \tau$) obtained by correcting the apparent shear rate $\dot{\gamma}'_w$ to the true shear rate $\dot{\gamma}$ using Eq. (4) is shown in the left side of Figure 4. In this manner the true flow curves of all samples were obtained.

The variations of the true flow curves with PE content are shown in Figures 6(a)-(e). The flow curves of the blends locate between those of the components and gradually change from the character of PP to that of PE with increasing PE content. In the case where the MFI of PP is higher than that of PE (PPM/PEL and PPH/PEM), the slope of the flow curve scarcely depends on the composition, and the flow curve shifts in parallel with increasing PE content. In the case where the MFI of PP is

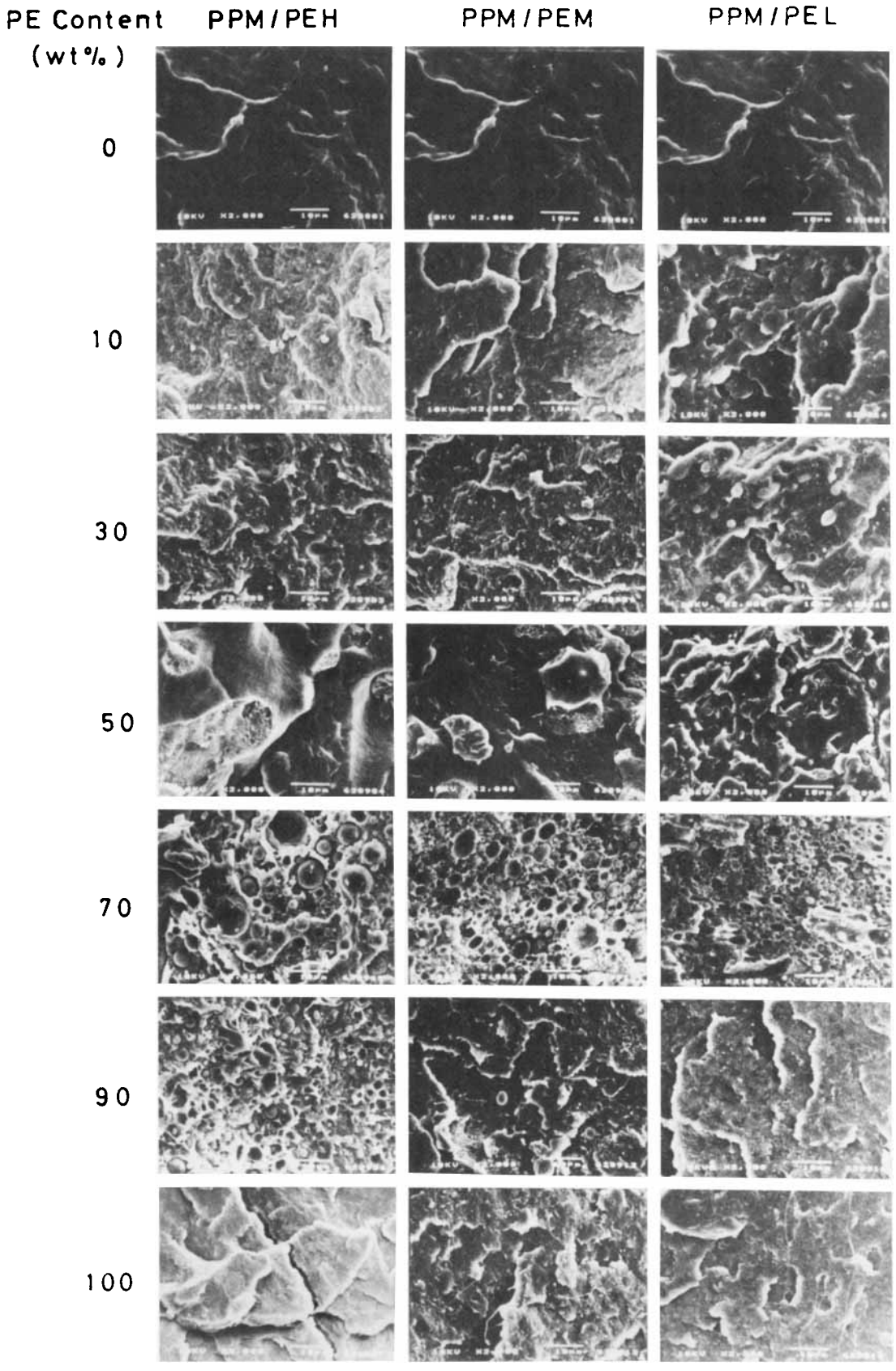

(a)

Figure 1 SEM photographs of cryogenic temperature-fractured surfaces of PP/HDPE blends. (a) PPM/PEH, PPM/PEM, and PPM/PEL systems. (b) PPH/PEM, PPM/PEM, and PPL/PEM systems.

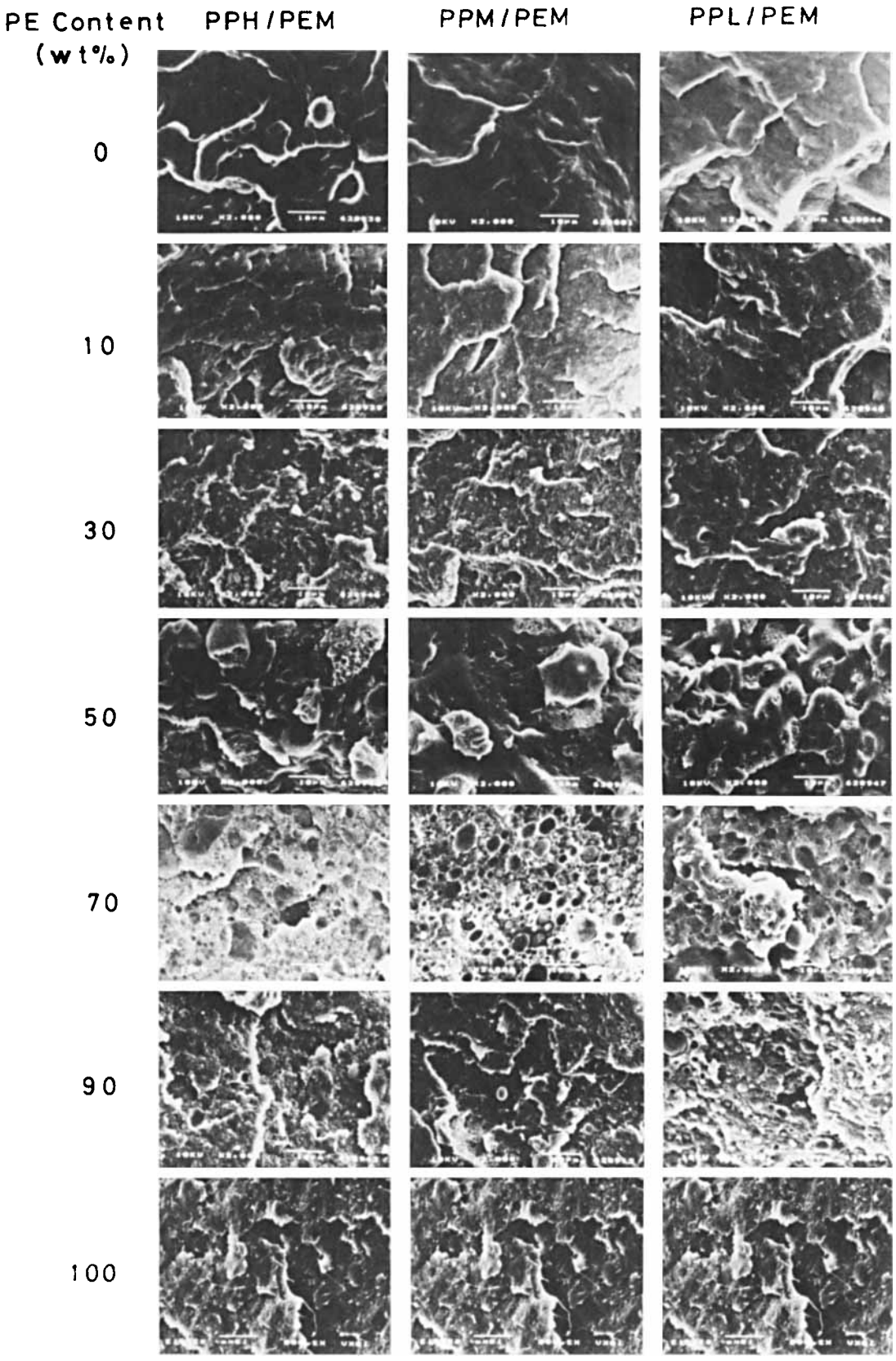

(b)

Figure 1 (*Continued from the previous page*)

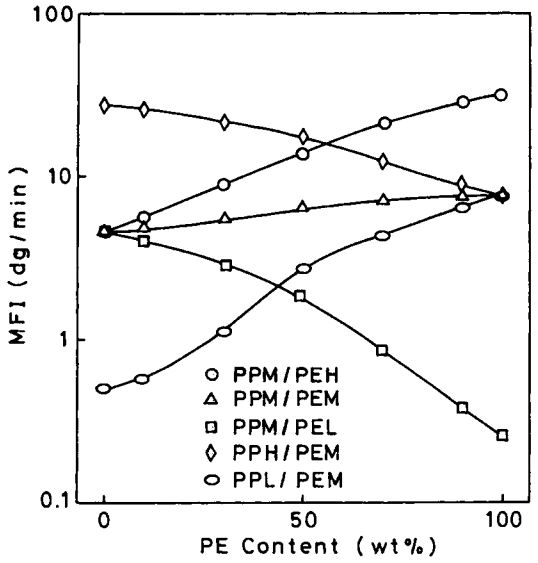

Figure 2 Dependence of MFI on PE content.

nearly equal to or lower than that of PE, the slope of the flow curve decreases with increasing PE content. Similar tendencies were reported by Hayashida et al.,[1] Plochocki,[2] Maciejewski and Griskey,[5] and Noel and Carley.[6] From these facts it can be said that the non-Newtonianity of HDPE is weaker than that of PP when compared on the same viscosity level. Discontinuities on the flow curves of PPM10/PEL90 and PPM0/PEL100 at high shear rate region in Figure 6(c) are due to the stick-slip phenomenon.

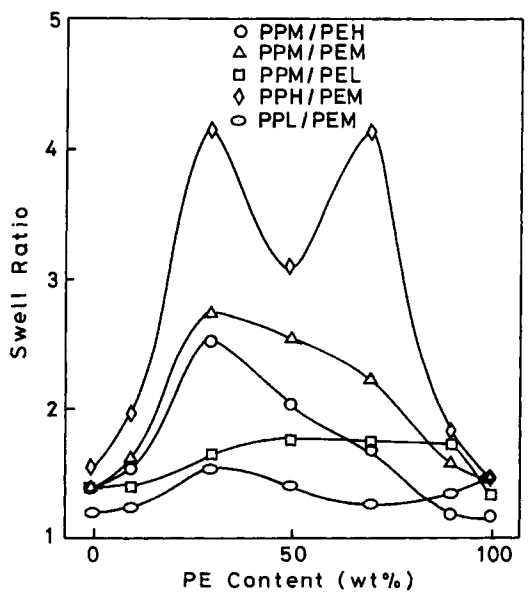

Figure 3 Dependence of die swell ratio on PE content.

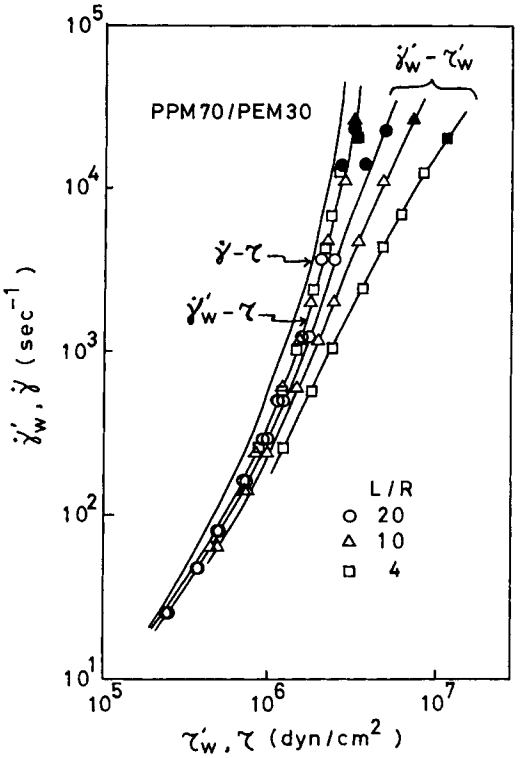

Figure 4 Flow curves for PPM70/PEM30 blend corrected at each stage.

Figure 7 shows the dependence of viscosities η at definite shear rates on PE content. The difference of η of each sample decreases with increasing shear rate. η's of the blends show negative deviations from

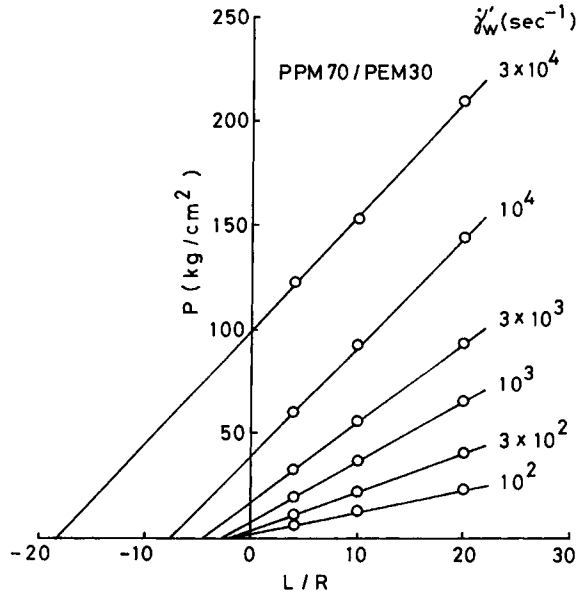

Figure 5 Bagley plots for PPM70/PEM30 blend.

logarithmic additivity except for PPM/PEH system, and the degree of the deviation increases with increasing shear rate. The deviation is especially large in the range of high PE content. The fact that the viscosities of blends show negative deviations from logarithmic additivity has been reported by many researchers.[1-6,8,13]

Entrance Effect

Figures 8(a)-(e) show the variations of the end correction coefficient ν with apparent shear rate $\dot{\gamma}'_w$ using PE content as a parameter. ν increases with increasing $\dot{\gamma}'_w$. ν's of the blends locate between those of the components and gradually change from the character of PP to that of PE with increasing PE content. The fact that the end correction coefficients of polymer blends locate between those of the components and gradually change from the character of one component to that of the other component, with increasing the other component has been reported on HDPE/low-density polyethylene (LDPE) blends by Curto et al.[32] and LDPE/linear low-density polyethylene (LLDPE) blends by Acierno et al.[33] Except for PPM/PEL, ν of HDPE is lower than that of PP, and ν of the blend decreases with increasing PE content. Since the end correction coefficient is a measure of melt elasticity, it can be said that the melt elasticity of HDPE is lower than that of PP. The fact that ν of PEL is similar to or slightly higher than that of PPM as shown in Figure 8(c) is considered to be because the molecular weight distribution of PEL is very broad as shown in Table I. Discontinuities on the ν vs. $\dot{\gamma}'_w$ curves of PPM10/PEL90 and PPM0/PEL100 at high shear rate region in Figure 8(c) are due to the stick-slip phenomenon.

Barus Effect

Figures 9(a)-(e) show the variations of die swell ratio D/D_0 with apparent shear rate $\dot{\gamma}'_w$ using PE content as a parameter. In general, the die swell ratios of thermoplastic resins increase monotonously with increasing shear rate except for poly(vinyl chloride) whose variation of die swell ratio with shear rate sometimes shows a maximum or a minimum. The die swell ratio vs. shear rate curves of PP/HDPE blends in this experiment show very complex features where maxima and/or minima appear according to the combination of the components. A tendency is obvious where the blends show higher die swell ratios than the components. Although this tendency is weak in PPM/PEL and PPL/PEM systems where the viscosity of either component is very high (below 1 decigram/min in MFI), it is notable in other blend systems. In particular, there are cases in PPH/PEM where the die swell ratio reaches an abnormally high value of about 5.

Figures 10(a) and (b) show the dependence of the die swell ratios at a definite shear rate $\dot{\gamma}'_w = 10^2$ s^{-1} and at a definite shear stress $\tau = 3 \times 10^5$ dyn/cm^2 on PE content, respectively. Both figures show a similar tendency. In the case where the viscosity of either component is very high (below 1 dg/min in MFI), to be concrete, in PPM/PEL and PPL/PEM systems, the die swell ratios of the blends scarcely differ from those of the components. In the case where the viscosities of the components are not so high, the die swell ratio shows one or two peaks at PE contents of 30 and 70 wt %. In both cases the highest peak appears when the content of lower viscosity component is 30 wt % and forms the disperse phase. Maxima in the dependence of the die swell ratios of polymer blends on the composition have been reported on, in addition to PP/HDPE,[8,15] ionomer/ethylene-vinyl acetate copolymer (EVA),[34] HDPE/EVA,[35] polystyrene (PS)/HDPE,[36] PS/poly(methylmethacrylate),[37] HDPE/LDPE,[38] PP/LDPE,[39] and HDPE/ethylene-methacrylic acid copolymer.[40] Fujimura and Iwakura[34] found that the die swell ratios of ionomer/EVA blends showed two peaks at compositions of 30 and 70 wt % and conjectured that the abnormal behavior originated from the partial compatibility of the components. Partial compatibility of PP and HDPE has been proved by Kryszewski et al.[41] Han and Kim[42] found that, for HDPE/PS blends, HDPE particles were dispersed in PS medium at compositions of HDPE/PS = 25/75 and 50/50, and in these cases the viscosity was minimum and the first normal stress difference was maximum. They explained these phenomena by assuming that HDPE particles were deformed during flow and stored recoverable elastic energy. According to the theory of Han and Kim, elasticity should be more notable as the deformability of suspended particles is higher or the viscosity of suspended particles is lower. The present experimental results as shown in Figure 10 show that the die swell ratio is the highest at a composition of a lower viscosity component content of 30 wt %, supporting the theory of Han and Kim.

Bagley and Duffey[43] applied the rubber elasticity theory to polymer melt and showed that the die swell ratio D/D_0 is related to the recoverable shear strain γ_e through Eq. (7):

$$\gamma_e = [(D/D_0)^4 - (D/D_0)^{-2}]^{1/2} \qquad (7)$$

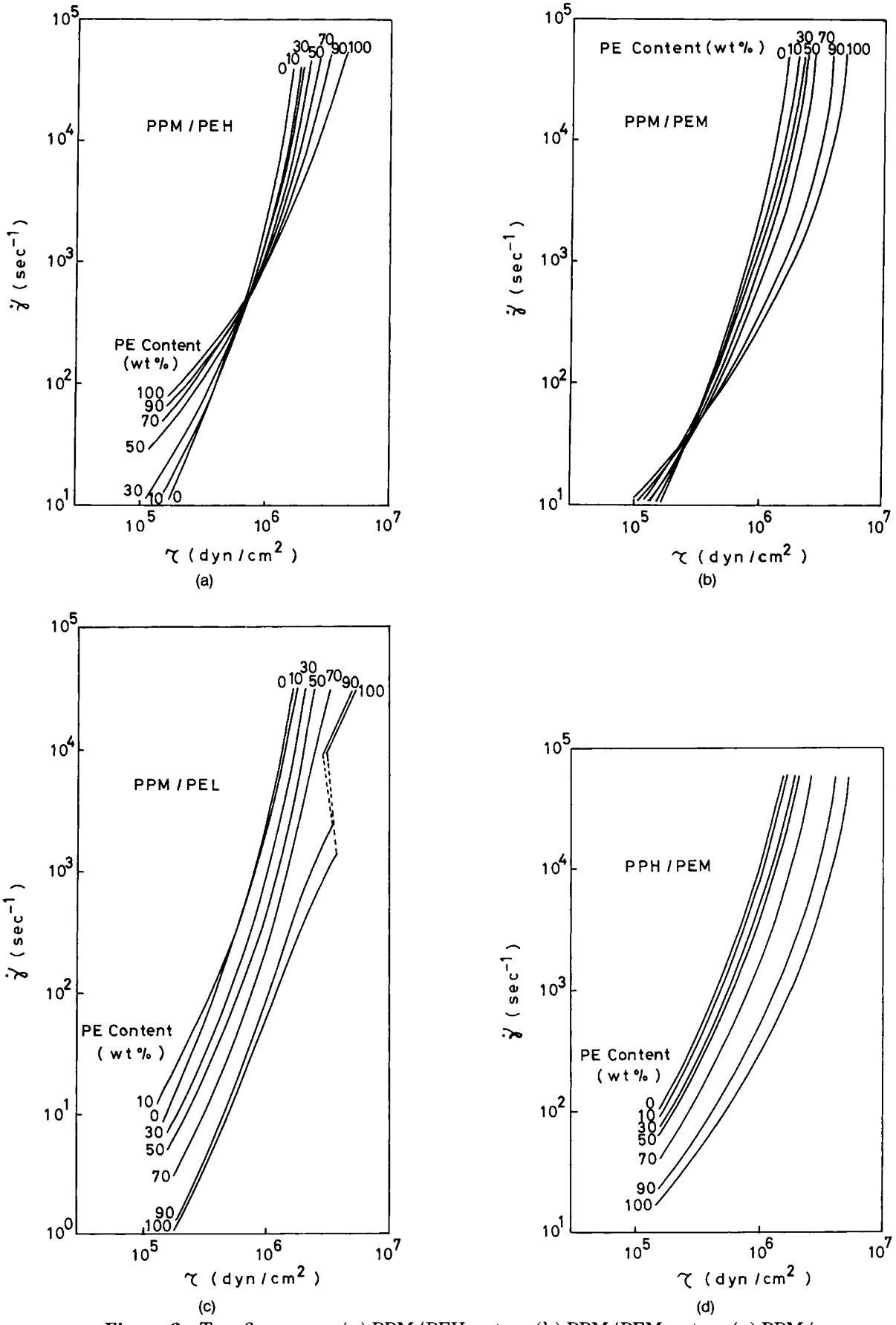

Figure 6 True flow curves. (a) PPM/PEH system. (b) PPM/PEM system. (c) PPM/PEL system. (d) PPH/PEM system. (e) PPL/PEM system.

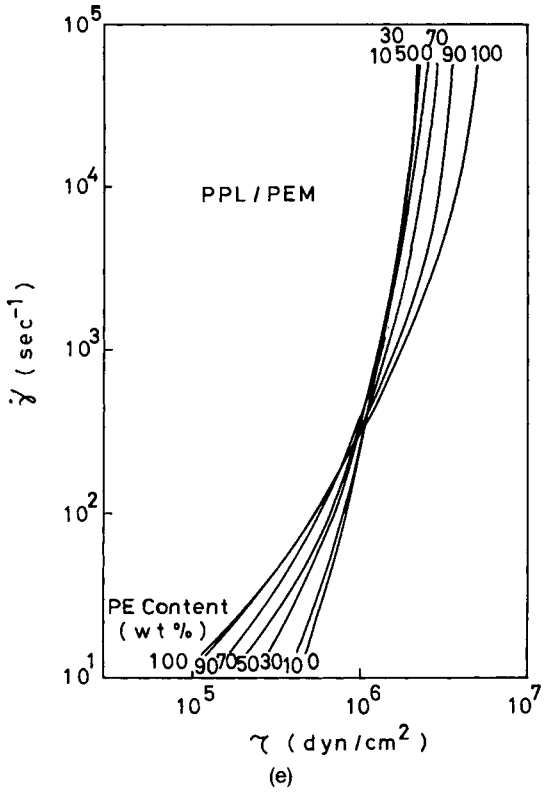

Figure 6 *(Continued from the previous page)*

Mendelson et al.[44] showed that Eq. (7) applied well to HDPE melts. On the other hand, Philippoff and Gaskins[45] related the end correction coefficient ν to the recoverable shear strain γ_e by Eq. (8):

$$\nu = n_c + \gamma_e/2 \tag{8}$$

where n_c is the Couette correction term and has a value of about 0.44.[46] The die swell ratio D/D_0 and the entrance correction coefficient ν is related through the recoverable shear strain γ_e using Eqs. (7) and (8) by Eq. (9):

$$\nu = n_c + \tfrac{1}{2}[(D/D_0)^4 - (D/D_0)^{-2}]^{1/2} \tag{9}$$

According to Eq. (9), there should exist a positive correlation between D/D_0 and ν. Actually, positive correlations have been reported on PP by Kamide and Fujii[47] and Fujiyama and Awaya,[48] on PS, PP, LDPE, and HDPE by Kishi and Iizuka,[49] and on concentrated dibutyl phthalate solution of PS by Shishido and Ito.[50]

In the case of PP/HDPE blends in the present experiment, the end correction coefficients ν of the blends locate between those of the components and gradually change with the composition as shown in Figure 8. On the other hand, the die swell ratios D/D_0 of the blends are higher than those of the components as shown in Figures 9 and 10. There is no correlation between D/D_0 and ν. Although in the case of homogeneous polymer melt both the die swell ratio D/D_0 and the end correction coefficient ν are measures of melt elasticity in capillary flow, it is not always appropriate to regard the end correction coefficient as a measure of melt elasticity in the case of inhomogeneous systems such as PP/HDPE blend.

Melt Fracture

Melt fractures occur at the closed points on the flow curves in Figure 4. The critical shear rate $\dot{\gamma}_c$ and the critical shear stress τ_c at which the melt fracture begins to occur were averaged over the respective values obtained with three dies of different L/R. For highly fluid samples, since the melt fracture did not occur in the experimental range, $\dot{\gamma}_c$ and τ_c could not be determined.

Figure 11 shows the dependence of the critical shear rates $\dot{\gamma}_c$ on PE content. In the case where the MFI of either component is very low (MFI < 1 dg/min), $\dot{\gamma}_c$'s show negative deviations from logarithmic additivity. In other cases, $\dot{\gamma}_c$'s show positive deviations. Valenza et al.[16] reported that $\dot{\gamma}_c$'s of PP/HDPE blends showed positive deviations from logarithmic additivity. Acierno et al.[51] reported that $\dot{\gamma}_c$'s of HDPE/LDPE blends showed complex variations with the composition where positive and negative deviations appeared according to the combination of MFIs of the components. Acierno et al.[33]

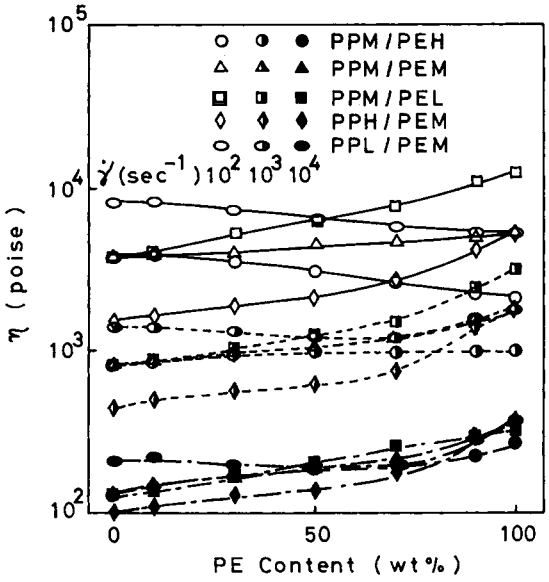

Figure 7 Dependence of viscosities η at definite shear rates.

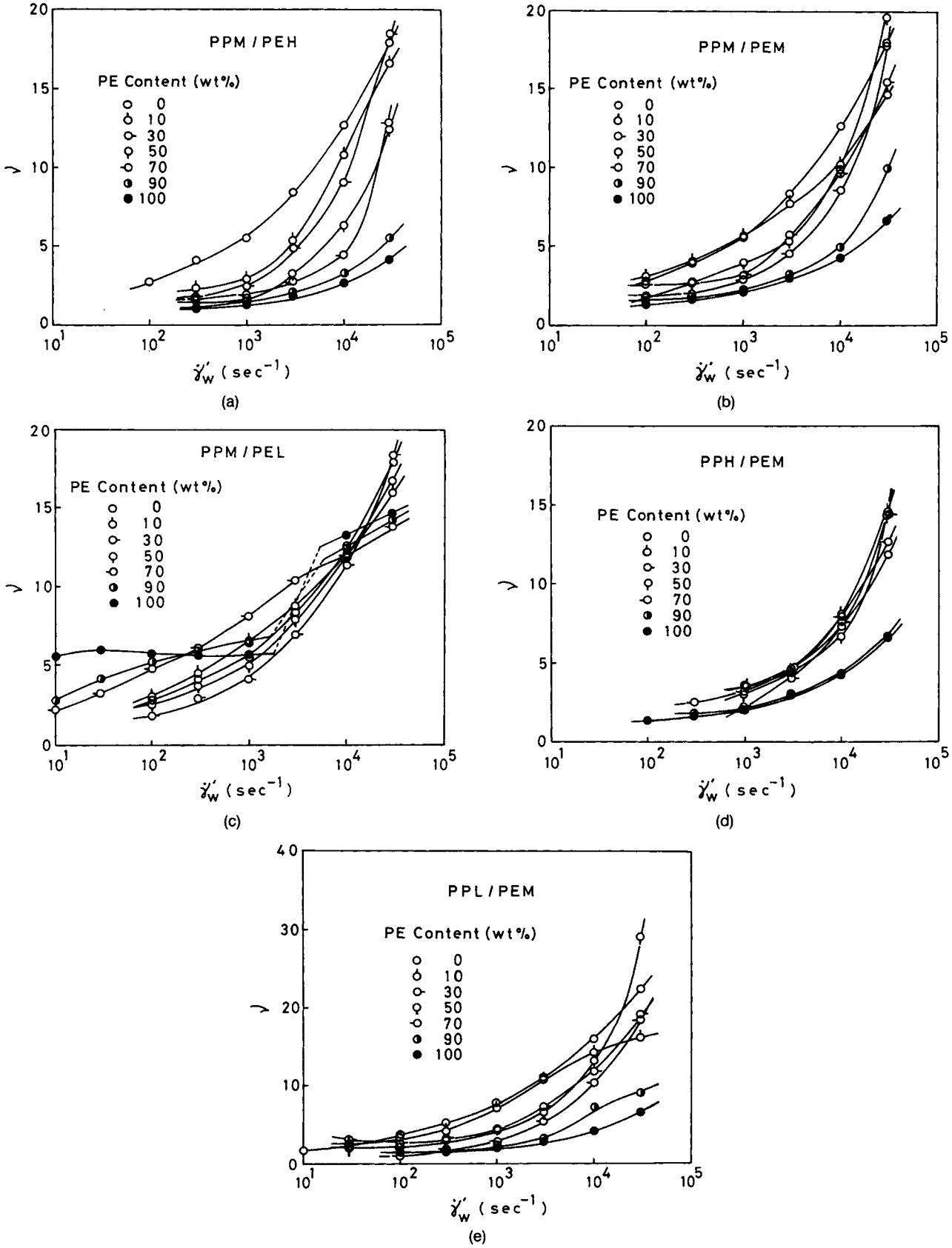

Figure 8 Variations of end correction coefficient ν with apparent shear rate $\dot{\gamma}'_w$. (a) PPM/PEH system. (b) PPM/PEM system. (c) PPM/PEL system. (d) PPH/PEM system. (e) PPL/PEM system.

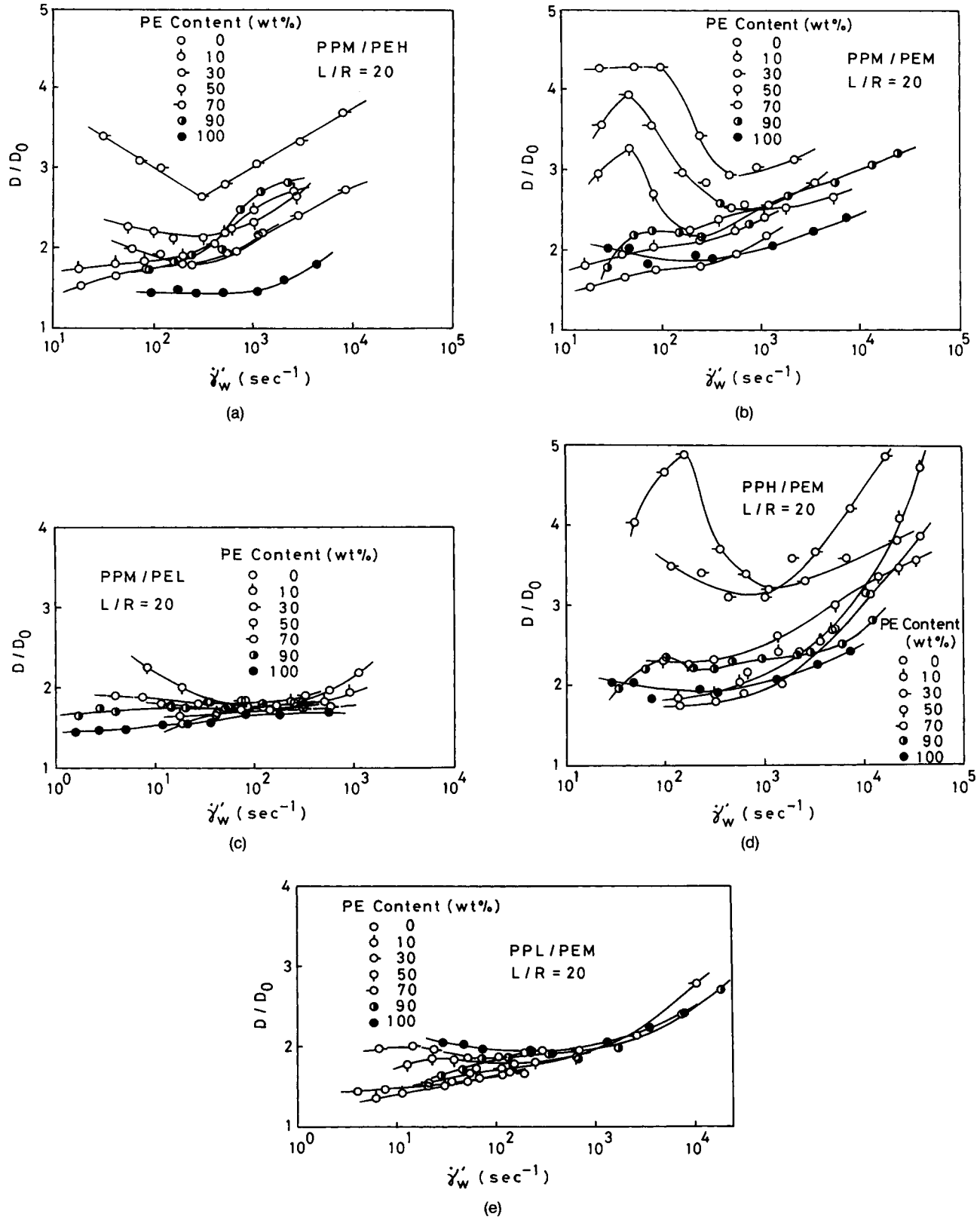

Figure 9 Variations of die swell ratio D/D_0 with apparent shear rate $\dot{\gamma}'_w$. (a) PPM/PEH system. (b) PPM/PEM system. (c) PPM/PEL system. (d) PPH/PEM system. (e) PPL/PEM system.

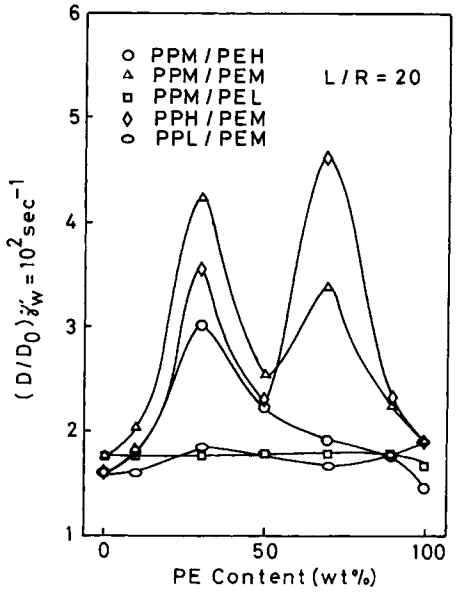

(a)

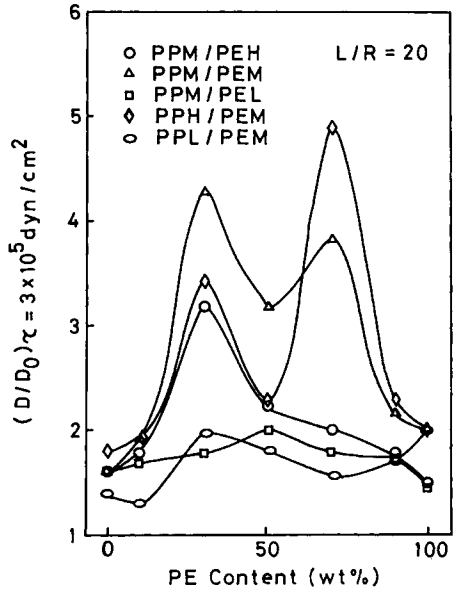

(b)

Figure 10 (a) Dependence of die swell ratio D/D_0 at apparent shear rate $\dot{\gamma}'_w = 10^2\ s^{-1}$ on PE content. (b) Dependence of die swell ratio at shear stress $\tau = 3 \times 10^5$ dyn/cm^2 on PE content.

reported that $\dot{\gamma}_c$'s of HDPE/LLDPE blends showed positive deviations. As already mentioned, no regular tendency has so far been found on the dependence of the critical shear rate $\dot{\gamma}_c$ of polymer blend on the composition.

Figure 12 shows the dependence of the critical shear stresses τ_c on PE content. Except for two points (PPH10/PEM90 and PPL10/PEM90), τ_c's of the blends locate between those of the components and

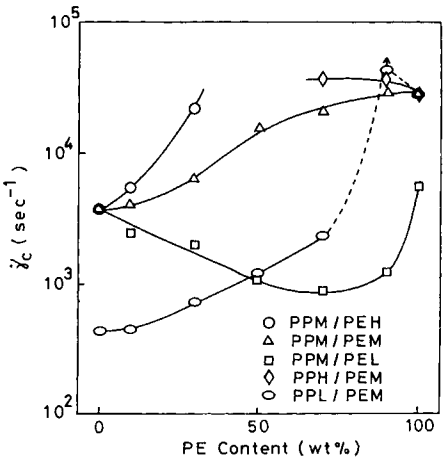

Figure 11 Dependence of critical shear rate $\dot{\gamma}_c$ on PE content.

show negative deviations from additivity. Noel and Carley[6] reported that τ_c's of PP/HDPE blends located between those of the components and showed a negative deviation, agreeing with the present experiment. Acierno et al.[51] reported that τ_c's of HDPE/LDPE blends located between those of the components and showed positive and negative deviations according to the combination of MFIs of the components. Acierno et al.[34] reported that τ_c's of LDPE/LLDPE blends located between those of the components and showed a positive deviation. The results of all researchers agree on the point that τ_c's of blends locate between those of the components.

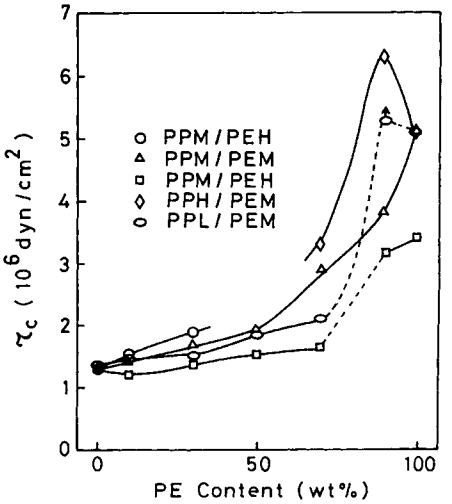

Figure 12 Dependence of critical shear stress τ_c on PE content.

CONCLUSIONS

Three kinds of isotactic polypropylenes (PP) with different MFI were melt-blended with three kinds of high-density polyethylenes (HDPE) with different MFI using a screw extruder and the morphologies and the capillary flow properties were studied. The following results were obtained:

1. When HDPE contents are 70 wt % or above and PP particles form the disperse phase, the particle size decreases with decreasing viscosity of PP. When HDPE contents are 30 wt % or below and HDPE particles form the disperse phase, the particle size is minimum when the viscosities of PP and HDPE are similar.
2. The flow curves of blends locate between those of the components and gradually change from that of one component to that of the other component with increasing the other component. Compared on the same viscosity level, the non-Newtonianity of HDPE is weaker than that of PP. The shear viscosities η of the blends show negative deviations from logarithmic additivity, and the deviations are more notable as the shear rate is higher.
3. The end correction coefficients ν of the blends locate between those of the components and change gradually from that of one component to that of the other component with increasing the other component.
4. The die swell ratios D/D_0 of the blends change in complex manners with shear rate showing maxima and/or minima according to the combination of the components. The D/D_0's of the blends show higher values than those of the components, and the dependence on the composition shows one or two peaks at HDPE contents of 30 and 70 wt % except for the cases where either component has very high viscosity. In both cases the highest peak appears when the content of lower viscosity component is 30 wt % and forms the disperse phase. D/D_0 reaches an abnormally high value of about 5 in some cases. Although in the case of homogeneous polymer melt both the die swell ratio D/D_0 and the end correction coefficient ν are measures of melt elasticity, it is not always appropriate to regard ν as a measure of melt elasticity in the case of inhomogeneous systems such as PP/HDPE blend since no correlation is observed between D/D_0 and ν.
5. The critical shear rates $\dot{\gamma}_c$ of the blends at which melt fractures begin to occur show negative deviations from logarithmic additivity when the MFI of either component is very low (MFI < 1 decigram/min) and positive deviations in other cases. The critical shear stresses τ_c of the blends locate between those of the components and show negative deviations.

REFERENCES

1. K. Hayashida, J. Takahashi, and M. Matsui, *Proceedings of the Fifth International Congress on Rheology*, **4**, 525 (1979).
2. A. Plochocki, *J. Appl. Polym. Sci.*, **16**, 987 (1972).
3. M. Kasajima and Y. Mori, *Chem. Eng., Jpn.*, **37**, 915 (1973).
4. M. Kasajima, A. Suganuma, D. Kunii, and K. Ito, *Kobunshi Ronbunshu*, **36**, 481 (1979).
5. K. Maciejewski and R. G. Griskey, *SPE Tech. Pap.*, 32nd. ANTEC, 23 (1974).
6. F. Noel, III and J. F. Carley, *Polym. Eng. Sci.*, **15**, 117 (1975).
7. A. P. Plochocki, *Trans. Soc. Rheol.*, **20**(2), 287 (1976).
8. V. F. Shumskii, Y. V. Lebedev, and Y. S. Lipatov, *Vysokomol Soyed.*, **A21**, 992 (1979).
9. N. Alle and J. Lyngaae-Jørgensen, *Rheol. Acta*, **19**, 94 (1980).
10. N. Alle and J. Lyngaae-Jørgensen, *Rheol. Acta*, **19**, 104 (1980).
11. N. Alle, F. F. Andersen, and J. Lyngaae-Jørgensen, *Rheol. Acta*, **20**, 222 (1981).
12. T. Nishimura, T. Sakai, and T. Kataoka, *Kobunshi Ronbunshu*, **38**, 223 (1981).
13. K. Murata, K. Nakashima, K. Funatsu, and H. Shinohara, *Kagakukogaku Ronbunshu*, **7**, 549 (1981).
14. A. P. Plochocki, *Polym. Eng. Sci.*, **27**, 1153 (1982).
15. M. Kasajima and M. Itoh, *Polym. Prepr., Jpn.*, **32**(10), 3025 (1983).
16. A. Valenza, F. P. La Mantia, and D. Acierno, *Eur. Polym. J.*, **20**, 727 (1984).
17. T. Nishimura, *Rheol. Acta*, **23**, 617 (1984); H. Sakai and T. Nishimura, *Repts. Indust. Res. Inst. Nagoya*, **4**(5), 21 (1985).
18. E. B. Bagley, *J. Appl. Phys.*, **28**, 624 (1957).
19. B. Z. Rabinowitsch, *Z. Physik. Chem. (Leipzig)*, **A145**, 1 (1929).
20. M. H. Walters and D. N. Keyte, *Trans. Proc. Inst. Rubber Ind. (Trans.)* **38**/9, 40 (1962).
21. W. M. Hess, C. E. Scott, and Y. E. Callan, *Rubber Chem. Tech.*, **40**, 371 (1967).
22. P. A. Marsh, A. Voet, L. D. Price, and T. J. Mullens, *Rubber Chem. Tech.*, **41**, 344 (1968).

23. V. N. Kuleznev, A. V. Grachev, and Y. P. Microshnikov, *Colloid J. USSR.*, **38,** 239 (1976).
24. O. Fukushima and K. Kogame, *Sen-i Gakkaishi,* **39,** 452 (1983).
25. S. Wu, *Polym. Eng. Sci.,* **27,** 335 (1987).
26. B. D. Favis and J. P. Chafloux, *Polym. Eng. Sci.,* **27,** 1591 (1987).
27. S. Maeda and T. Masuda, The Fifth Annual Meeting, PPS, 223 (1989).
28. J. M. Starita, *Trans. Soc. Rheol.,* **16,** 339 (1972).
29. S. Danesi and R. S. Porter, *Polymer,* **19,** 448 (1978).
30. J. Karger-Kocsis, A. Kalló, and V. N. Kuleznev, *Acta Polym.,* **32,** 578 (1981).
31. W. Berger, H. W. Kammer, and C. Kummerlöwe, *Makromol. Chem., Suppl.,* **8,** 101 (1984).
32. D. Curto, F. P. La Mantia, and D. Acierno, *Rheol. Acta,* **22,** 197 (1983).
33. D. Acierno, D. Curto, F. P. La Mantia, and A. Valenza, *Polym. Eng. Sci.,* **26,** 28 (1986).
34. T. Fujimura and K. Iwakura, *Sen-i Gakkaishi,* **26,** 455 (1970).
35. T. Fujimura and K. Iwakura, *Kogyo Kagaku Zasshi,* **73,** 1641 (1970).
36. C. D. Han and T. C. Yu, *AIChE J.* **17,** 1512 (1971).
37. J. Lyngaae-Jørgensen, F. E. Andersen, and N. Alle, *Polym. Sci. Tech.,* **20,** 105 (1983).
38. F. P. La Mantia, D. Curto, and D. Acierno, *Acta Polymerica,* **35**(1), 71 (1984).
39. A. Santamaria, M. E. Muñoz, J. J. Peña, and P. Remiro, *Angew. Makromol. Chem.,* **134,** 63 (1985).
40. K. Iwakura and K. Saito, *Polym. Prepr., Jpn.,* **35**(4), 819 (1986); K. Saito, K. Yoshida, K. Iwakura, and T. Masuko, *Polym. Prepr., Jpn.,* **36**(4), 1270 (1987).
41. M. Kryszewski, A. Galeski, T. Pakula, and J. Grobowicz, *J. Colloid Interf. Sci.,* **44,** 85 (1973).
42. C. D. Han and Y. W. Kim, *Trans. Soc. Rheol.,* **19**(2), 245 (1975).
43. E. B. Bagley and H. J. Duffey, *Trans. Soc. Rheol.,* **14**(4), 545 (1970).
44. R. A. Mendelson, F. L. Finger, and E. B. Bagley, *J. Polym. Sci., Part C,* **35,** 177 (1971).
45. W. Philippoff and F. H. Gaskins, *Trans. Soc. Rheol.,* **2,** 263 (1958).
46. Y. Tomita, *Nihon Kikaigakkai Ronbunshu (Part 3),* **25,** 938 (1959).
47. K. Kamide and K. Fujii, *Kobunshi Kagaku,* **24,** 120 (1967).
48. M. Fujiyama and H. Awaya, *J. Appl. Polym. Sci.,* **16,** 275 (1972).
49. N. Kishi and H. Iizuka, *J. Polym. Sci., Part B2,* **2,** 399 (1964).
50. S. Shishido and Y. Ito, *Nihon Kagaku Zasshi,* **85,** 191 (1964).
51. D. Acierno, F. P. La Mantia, and D. Curto, *Polym. Bull.,* **11,** 223 (1984).

Received October 31, 1989
Accepted March 8, 1990